Electromagnetic Scattering by Arbitrary Shaped Three-Dimensional Conducting Objects Covered with Electromagnetic Anisotropic Materials

Xiaoqiao Deng, Changqing Gu, and Yonggang Zhou

College of Information Science and Technology, Nanjing University of Aeronautics and Astronautics, Nanjing, 210016, China
dengxiaoqiao_521@163.com, gucq0138@sina.com, iamrealzyg@yahoo.com.cn

Abstract ─ In this paper, the equivalent dipole-moment method (EDM) is extended and applied in the analysis of electromagnetic (EM) scattering by the arbitrarily shaped perfect electric conductor (PEC) targets coated with EM anisotropic media. At first, the volume integral equation and surface integral equation are built in the EM anisotropic material region and on the conducting surface, respectively. Then, the method of moments (MoM) is used to convert the integral equation into a matrix equation and the EDM is employed to reduce the CPU time of the matrix filling procedure. Numerical results are given to demonstrate the versatility of the proposed approach in handing with the EM scattering by arbitrarily shaped PEC targets coated with EM anisotropic media.

Index Terms ─ Equivalent dipole moment (EDM), EM anisotropic material, method of moments (MOM), radar cross section (RCS), volume-surface integral equation (VSIE).

I. INTRODUCTION

EM scattering from composite bodies consisting of both conductor and coated anisotropic medium is an important and challenging problem in computational electromagnetics. Many effective methods have been proposed, among which the physical optics (PO) method [1], the finite difference time domain FDTD method [2], and the MoM [3] are used commonly. However, the PO solution is approximate and show bigger error when solving the EM scattering from coated targets. FDTD has significant accumulated errors from numerical dispersion. The MoM and its accelerated methods can overcome these disadvantages and many previous works [3-10] have been done to investigate the scattering problems of composite bodies consisting of both conductor and coated anisotropic medium.

However, when computing the impedance matrix elements, the conventional MoM consumes a considerable portion of the total solution time and memory. Moreover, this problem becomes even more serious in the analysis of anisotropic media. In recent researches, the EDM [11-12] based on the volume-surface integration equations (VSIE) has been put forward to compute the RCSs of arbitrarily shaped PEC targets coated with electric anisotropic media. It is demonstrated that the EDM can save matrix-filling time efficiently. However, in [11-12], only electric anisotropic media is considered. In many applications, such as stealth materials, both electric and magnetic anisotropic media are often used. So, in this paper, the equivalent dipole-moment method is extended and applied to model arbitrary targets covered by arbitrary electric and magnetic anisotropic media.

The article is organized as follows: Section II presents the MOM associated with VSIE and introduces the EDM in detail for 3-D arbitrary shaped conducting objects covered with EM anisotropic materials, respectively; numerical results are given in Sections III and some conclusions are drawn in the final section.

II. FORMULATIONS

A. Introduction of VSIE and MOM

For generalizing the proposed method, we refer to scattering from an arbitrary shaped 3-D conducting object coated with anisotropic media, shown in Fig. 1. Region V is an anisotropic medium characterized by relative permittivity $\bar{\bar{\varepsilon}}_r$ and permeability $\bar{\bar{\mu}}_r$ as:

Submitted On: May 16, 2011
Accepted On: Oct. 21, 2011

1054-4887 © 2011 ACES

$$\overline{\overline{\varepsilon}}_r = \begin{bmatrix} \varepsilon_{xx} & \varepsilon_{xy} & \varepsilon_{xz} \\ \varepsilon_{yx} & \varepsilon_{yy} & \varepsilon_{yz} \\ \varepsilon_{zx} & \varepsilon_{zy} & \varepsilon_{zz} \end{bmatrix}, \overline{\overline{\mu}}_r = \begin{bmatrix} \mu_{xx} & \mu_{xy} & \mu_{xz} \\ \mu_{yx} & \mu_{yy} & \mu_{yz} \\ \mu_{zx} & \mu_{zy} & \mu_{zz} \end{bmatrix}. \quad (1)$$

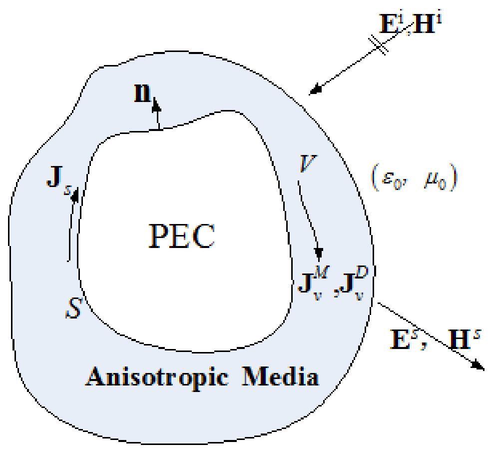

Fig. 1. Arbitrarily shaped conducting/anisotropic mixed body illuminated by a plane wave.

Let S denote the surface of a PEC object with unit normal vector n and the incident fields $\mathbf{E}^{i}, \mathbf{H}^{i}$ are due to an impressed source in the absence of the target. Hence, the EM field on the surface of the conducting object and in the volume of the anisotropic media must satisfy the equations below,

$$\mathbf{n}\times\left[\mathbf{E}^{i}+\mathbf{E}^{s}\left(\mathbf{J}_{s}\right)+\mathbf{E}^{s}\left(\mathbf{J}_{v}^{D}\right)+\mathbf{E}^{s}\left(\mathbf{J}_{v}^{M}\right)\right]=0, \quad \text{on S} \quad (2)$$

$$\mathbf{E}=\mathbf{E}^{i}+\mathbf{E}^{s}\left(\mathbf{J}_{s}\right)+\mathbf{E}^{s}\left(\mathbf{J}_{v}^{D}\right)+\mathbf{E}^{s}\left(\mathbf{J}_{v}^{M}\right), \quad \text{in V} \quad (3)$$

$$\mathbf{H}=\mathbf{H}^{i}+\mathbf{H}^{s}\left(\mathbf{J}_{s}\right)+\mathbf{H}^{s}(\mathbf{J}_{v}^{D})+\mathbf{H}^{s}(\mathbf{J}_{v}^{M}), \quad \text{in V} \quad (4)$$

where $\mathbf{E}$ and $\mathbf{H}$ are the total electrical field and magnetic field. $\mathbf{E}^{s}\left(\mathbf{J}_{s}\right)$ and $\mathbf{H}^{s}\left(\mathbf{J}_{s}\right)$ are the scattered electric and magnetic field due to the surface polarization current $\mathbf{J}_{s}$ on the conducting surface. $\mathbf{E}^{s}\left(\mathbf{J}_{v}^{t}\right)$ and $\mathbf{H}^{s}\left(\mathbf{J}_{v}^{t}\right)\left(t=D,M\right)$ are the scattered electric and magnetic fields due to the volume polarization current $\mathbf{J}_{v}^{t}$ in the medium. Equations (3) and (4) are volume-integral equations (VIE), and equation (2) by setting the tangential electric field to zero on the conducting surface is the electric field surface-integral equation (SIE), these three equations constitute the coupled volume-surface integral equations (VSIE), which will be used for the numerical solution in this work.

The surface current $\mathbf{J}_{s}$ on S can be represented by vector basis functions RWG [13], namely

$$\mathbf{J}_{s}\approx\sum_{n=1}^{N_s} I_{s,n}^{J}\mathbf{f}_{s,n}(\boldsymbol{r}), \qquad \boldsymbol{r}\in S \qquad (5)$$

where $I_{s,n}^{J}$ is the unknown expansion coefficient, $\mathbf{f}_{s,n}$ represents the nth face basis function for the nth common edge and N_s is the total number of the common edges.

The volume electric current $\mathbf{J}_{v}^{\mathrm{D}}$ and magnetic current $\mathbf{J}_{v}^{\mathrm{M}}$ within V can be then expressed by vector basis function SWG [14] as

$$\mathbf{J}_{v}^{M}=\sum_{n=1}^{N_v} I_{v,n}^{M}\overline{\overline{\kappa}}^{m}(\mathbf{r})\cdot\left(\eta_0\mathbf{f}_{v,n}(\mathbf{r})\right), \qquad \mathbf{r}\in V \qquad (6)$$

$$\mathbf{J}_{v}^{M}=\sum_{n=1}^{N_v} I_{v,n}^{M}\overline{\overline{\kappa}}^{m}(\mathbf{r})\cdot\left(\eta_0\mathbf{f}_{v,n}(\mathbf{r})\right), \qquad \mathbf{r}\in V \qquad (7)$$

where $I_{v,n}^{D}$ and $I_{v,n}^{M}$ are the unknown expansion coefficients for the electric and magnetic currents in the dielectric volume, respectively. $\mathbf{f}_{v,n}$ denotes the basis function for the nth face of the tetrahedral model of V, and N_v is the number of common faces. $\overline{\overline{\kappa}}^{e}(\mathbf{r})$ and $\overline{\overline{\kappa}}^{m}(\mathbf{r})$ are the contrast ratio tensor defined by

$$\overline{\overline{\kappa}}^{e}(\mathbf{r})=(\overline{\overline{\varepsilon}}_r-\overline{\overline{I}})\cdot\overline{\overline{\varepsilon}}_r^{-1}, \qquad (8)$$

$$\overline{\overline{\kappa}}^{m}(\mathbf{r})=(\overline{\overline{\mu}}_r-\overline{\overline{I}})\cdot\overline{\overline{\mu}}_r^{-1}. \qquad (9)$$

It's necessary to note that the introduction of wave impedance η_0 is to achieve well conditioned systems and accurate solutions.

Using the extended Galerkin's method and substituting the equations (5), (6), and (7) into (2), (3), and (4), respectively, we can test (2) with the surface basis function $\mathbf{f}_{s,m}$, (3) with the volume basis function $\mathbf{f}_{v,m}$, and (4) with the volume basis function $\eta_0\mathbf{f}_{v,m}$. And finally a linear system consisting of N_s+2N_v independent equations is obtained, which can be written in a matrix form as

$$\begin{bmatrix} \boldsymbol{Z}^{JJ} & \boldsymbol{Z}^{JD} & \eta_0\boldsymbol{Z}^{JM} \\ \boldsymbol{Z}^{DJ} & \boldsymbol{Z}^{DD} & \eta_0\boldsymbol{Z}^{DM} \\ \eta_0\boldsymbol{Z}^{MJ} & \eta_0\boldsymbol{Z}^{MD} & \eta_0{}^{2}\boldsymbol{Z}^{MM} \end{bmatrix}\begin{bmatrix} \boldsymbol{I}^{J} \\ \boldsymbol{I}^{D} \\ \boldsymbol{I}^{M} \end{bmatrix}=\begin{bmatrix} \boldsymbol{V}^{J} \\ \boldsymbol{V}^{D} \\ \eta_0\boldsymbol{V}^{M} \end{bmatrix}, \qquad (10)$$

where $\boldsymbol{Z}^{JJ}$, $\boldsymbol{Z}^{JD}$, $\boldsymbol{Z}^{JM}$, $\boldsymbol{Z}^{DJ}$, $\boldsymbol{Z}^{DD}$, $\boldsymbol{Z}^{DM}$, $\boldsymbol{Z}^{MJ}$, $\boldsymbol{Z}^{MD}$, and $\boldsymbol{Z}^{MM}$ are the impedance sub-matrices with the dimension of $N_s \times N_s$, $N_s \times N_v$, $N_s \times N_v$, $N_v \times N_s$, $N_v \times N_v$, $N_v \times N_v$, $N_v \times N_s$, $N_v \times N_v$ and $N_v \times N_v$. $\boldsymbol{I}^J$ is the column vector of length N_s, while $\boldsymbol{I}^D$ and $\boldsymbol{I}^M$ are column vectors of length N_v. Similarly, $\boldsymbol{V}^J$ is the column vector of length N_s, while $\boldsymbol{V}^D$ and $\boldsymbol{V}^M$ are column vectors of length N_v. Then, we can obtain the entries of the impendence matrix blocks as

$$Z_{mn}^{JJ} = -< \mathbf{f}_{s,m}, \mathbf{E}^s\left(\mathbf{f}_{s,n}\right)>, \ m,n = 1,2\cdots N_s, \tag{11}$$

$$Z_{mn}^{JD} = -< \mathbf{f}_{s,m}, \mathbf{E}^s\left(\overline{\overline{\kappa}}^e \cdot \mathbf{f}_{v,n}\right)>, \ m = 1,2\cdots N_s, \ n = 1,2\cdots N_v, \tag{12}$$

$$Z_{mn}^{JM} = -< \mathbf{f}_{s,m}, \mathbf{E}^s\left(\overline{\overline{\kappa}}^m \cdot \mathbf{f}_{v,n}\right)>, \ m = 1,2\cdots N_s, \ n = 1,2\cdots N_v, \tag{13}$$

$$Z_{mn}^{DJ} = -< \mathbf{f}_{v,m}, \mathbf{E}^s\left(\mathbf{f}_{s,n}\right)>, \ m = 1,2,\cdots N_v, \ n = 1,2,\cdots N_s, \tag{14}$$

$$Z_{mn}^{DD} = < \mathbf{f}_{v,m}, \frac{\overline{\overline{\varepsilon}}_r^{-1} \cdot \mathbf{f}_{v,n}}{j\omega\varepsilon_0} > - < \mathbf{f}_{v,m}, \mathbf{E}^s\left(\overline{\overline{\kappa}}^e \cdot \mathbf{f}_{v,n}\right)>, \ m,n = 1,2,\cdots N_v, \tag{15}$$

$$Z_{mn}^{DM} = -< \mathbf{f}_{v,m}, \mathbf{E}^s\left(\overline{\overline{\kappa}}^m \cdot \mathbf{f}_{v,n}\right)>, \ m,n = 1,2,\cdots N_v, \tag{16}$$

$$Z_{mn}^{MJ} = -< \mathbf{f}_{v,m}, \mathbf{H}^s\left(\mathbf{f}_{s,n}\right)>, \ m = 1,2,\cdots N_v, \ n = 1,2,\cdots N_s, \tag{17}$$

$$Z_{mn}^{MD} = -< \mathbf{f}_{v,m}, \mathbf{H}^s\left(\overline{\overline{\kappa}}^e \cdot \mathbf{f}_{v,n}\right)>, \ m,n = 1,2,\cdots N_v, \tag{18}$$

$$Z_{mn}^{MM} = < \mathbf{f}_{v,m}, \frac{\overline{\overline{\mu}}_r^{-1} \cdot \mathbf{f}_{v,n}}{j\omega\mu_0} > - < \mathbf{f}_{v,m}, \mathbf{H}^s\left(\overline{\overline{\kappa}}^m \cdot \mathbf{f}_{v,n}\right)>, \ m,n = 1,2,\cdots N_v. \tag{19}$$

The excitation column entries contain the following integrals:

$$V_m^J = \int_S dS \mathbf{f}_{s,m} \cdot \mathbf{E}^{\mathrm{i}}, \tag{20}$$

$$V_m^D = \int_V dV \mathbf{f}_{v,m} \cdot \mathbf{E}^{\mathrm{i}}, \tag{21}$$

$$V_m^M = \int_V dV \mathbf{f}_{v,m} \cdot \mathbf{H}^{\mathrm{i}}. \tag{22}$$

B. The application of EDM to accelerate the MOM

The conducting surface S is first meshed into triangles and each triangle pair can be represented by a RWG element, the medium V can also be discretized into tetrahedrons and each tetrahedron pair can be represented by a SWG element. The nth face electric dipole moment $\mathbf{m}_n^J$ corresponds to a pair of triangle patches, the nth volume electric dipole moment $\mathbf{m}_n^D$ corresponds to tetrahedrons and their scattered fields can be found in [12]. The nth volume magnetic dipole moment can be written as

$$\mathbf{m}_n^M = \begin{cases} a_{v,n}\overline{\overline{\kappa}}^m \bullet (\mathbf{r}_{v,n}^{c-} - \mathbf{r}_{v,n}^{c+}) & T_{v,n}^{\pm} \in V \\ a_{v,n}\overline{\overline{\kappa}}^m \bullet (\mathbf{r}_{ns}^{c} - \mathbf{r}_{v,n}^{c+}) & T_{v,n}^{+} \in V \text{ and } T_{v,n}^{-} \notin V \end{cases}. \tag{23}$$

Here, $\mathbf{r}_{v,n}^{c\pm}$ and $\mathbf{r}_{ns}^{c}$ are the centroid radius vector of a pair of tetrahedrons $T_{v,n}^{\pm}$ and the *n*th boundary face, respectively. $a_{v,n}$ is the area of the common face associated with $T_{v,n}^{\pm}$ or the area of the *n*th boundary face associated with $T_{v,n}^{+}$. Referring to [12] and electric-magnetic duality, the scattered fields of the nth infinitesimal magnetic dipole at the centroid radius vector $\mathbf{r}_{u,m}\left(u = s, v\right)$ are

$$\mathbf{E}^s\left(\mathbf{m}_n^M\right) = -\frac{jk}{4\pi}\left(\mathbf{m}_n^M \times \mathbf{R}\right) C e^{-jkR}\Big|_{R=\left|\mathbf{r}_{u,m} - \mathbf{r}'_{v,n}\right|}, \tag{24}$$

$$\mathbf{H}^s\left(\mathbf{m}_n^M\right) = \frac{1}{4\pi\eta}\left[\left(\mathbf{M}_n^M - \mathbf{m}_n^M\right)\left(\frac{jk}{R} + C\right) + 2\mathbf{M}_n^M C\right] e^{-jkR}\Big|_{R=\left|\mathbf{r}_{u,m} - \mathbf{r}'_{v,n}\right|}, \tag{25}$$

where $\boldsymbol{r}_{u,m}$ and $\boldsymbol{r}'_{v,n}$ are the center radius vectors of the *m*th and the *n*th equivalent dipole model, respectively.

$$C = \frac{1}{R^2}\left[1 + \frac{1}{jkR}\right] \tag{26}$$

and

$$\mathbf{M}_n^M = \frac{\left(\mathbf{R} \cdot \mathbf{m}_n^M\right)\mathbf{R}}{R^2}. \tag{27}$$

Here, $\mathbf{R} = \mathbf{r}_{u,m} - \mathbf{r}'_{v,n}$ and $R = \left|\mathbf{R}\right|$. Equations (24) and (25) are the exact expressions and valid at arbitrary distances from the dipole. Considering the accuracy and efficiency of the algorithm, the critical distance between the source and the testing function locations is chosen as $0.15\lambda_g$, where λ_g is the wavelength in dielectric body [11-12]. The MOM matrix elements are computed by the EDM method directly for a separation distance of greater than the critical distance. Substituting (24) into (13) and (16), (25) into (17)-(19), and associated with paper [12], the expressions of the impedance matrix elements are calculated by

$$Z_{mn}^{JJ} = -l_{s.m}\mathbf{E}^s(\mathbf{m}_n^J) \cdot (\mathbf{r}_{s,m}^{c-} - \mathbf{r}_{s,m}^{c+}), \quad T_{s,m}^{\pm} \in S \tag{28}$$

$$Z_{mn}^{JD} = -l_{s.m}\mathbf{E}^s(\mathbf{m}_n^D) \cdot (\mathbf{r}_{s,m}^{c-} - \mathbf{r}_{s,m}^{c+}), \quad T_{s,m}^{\pm} \in S \tag{29}$$

$$Z_{mn}^{JM} = -l_{s.m}\mathbf{E}^s(\mathbf{m}_n^M) \cdot (\mathbf{r}_{s,m}^{c-} - \mathbf{r}_{s,m}^{c+}), \quad T_{s,m}^{\pm} \in S \tag{30}$$

$$Z_{mn}^{DJ}=\begin{cases}-a_{v,m}\mathbf{E}^s(\mathbf{m}_n^J)\cdot(\mathbf{r}_{v,m}^{c-}-\mathbf{r}_{v,m}^{c+}) & T_{v,m}^{\pm}\in V\\ -a_{v,m}\mathbf{E}^s(\mathbf{m}_n^J)\cdot(\mathbf{r}_{ms}^{c-}-\mathbf{r}_{v,m}^{c+}), & T_{v,m}^{+}\in V \text{ and } T_{v,m}^{-}\notin V\end{cases} \tag{31}$$

$$Z_{mn}^{DD}=\begin{cases}-a_{v,m}\mathbf{E}^s(\mathbf{m}_n^D)\cdot(\mathbf{r}_{v,m}^{c-}-\mathbf{r}_{v,m}^{c+}) & T_{v,m}^{\pm}\in V\\ -a_{v,m}\mathbf{E}^s(\mathbf{m}_n^D)\cdot(\mathbf{r}_{ms}^{c-}-\mathbf{r}_{v,m}^{c+}), & T_{v,m}^{+}\in V \text{ and } T_{v,m}^{-}\notin V\end{cases} \tag{32}$$

$$Z_{mn}^{DM}=\begin{cases}-a_{v,m}\mathbf{E}^s(\mathbf{m}_n^M)\cdot(\mathbf{r}_{v,m}^{c-}-\mathbf{r}_{v,m}^{c+}) & T_{v,m}^{\pm}\in V\\ -a_{v,m}\mathbf{E}^s(\mathbf{m}_n^M)\cdot(\mathbf{r}_{ms}^{c-}-\mathbf{r}_{v,m}^{c+}), & T_{v,m}^{+}\in V \text{ and } T_{v,m}^{-}\notin V\end{cases} \tag{33}$$

$$Z_{mn}^{MJ}=\begin{cases}-a_{v,m}\mathbf{H}^s(\boldsymbol{m}_n^J)\cdot(\mathbf{r}_{v,m}^{c-}-\mathbf{r}_{v,m}^{c+}) & T_{v,m}^{\pm}\in V\\ -a_{v,m}\mathbf{H}^s(\boldsymbol{m}_n^J)\cdot(\mathbf{r}_{ms}^{c-}-\mathbf{r}_{v,m}^{c+}), & T_{v,m}^{+}\in V \text{ and } T_{v,m}^{-}\notin V\end{cases} \tag{34}$$

$$Z_{mn}^{MD}=\begin{cases}-a_{v,m}\mathbf{H}^s(\boldsymbol{m}_n^D)\cdot(\mathbf{r}_{v,m}^{c-}-\mathbf{r}_{v,m}^{c+}) & T_{v,m}^{\pm}\in V\\ -a_{v,m}\mathbf{H}^s(\boldsymbol{m}_n^D)\cdot(\mathbf{r}_{ms}^{c-}-\mathbf{r}_{v,m}^{c+}), & T_{v,m}^{+}\in V \text{ and } T_{v,m}^{-}\notin V\end{cases} \tag{35}$$

$$Z_{mn}^{MM}=\begin{cases}-a_{v,m}\mathbf{H}_n^s(\boldsymbol{m}_n^M)\cdot(\mathbf{r}_{v,m}^{c-}-\mathbf{r}_{v,m}^{c+}) & T_{v,m}^{\pm}\in V\\ -a_{v,m}\mathbf{H}_n^s(\boldsymbol{m}_n^M)\cdot(\mathbf{r}_{ms}^{c-}-\mathbf{r}_{v,m}^{c+}), & T_{v,m}^{+}\in V \text{ and } T_{v,m}^{-}\notin V\end{cases} \tag{36}$$

where $l_{s.m}$ is the length of m^{th} common edge associated with a pair of triangle patches $T_{s,m}^{\pm}$ and $\mathbf{r}_{s,m}^{c\pm}$ is the centroid radius vector of $T_{s,m}^{\pm}$ [12].

Equations (28)-(36) are universal that it is unnecessary to treat the boundary condition on the surface of the mixed body, so the EDM method can be constructed by using a simple procedure and the impedance matrix's generation is very efficient. From the above equations, it can be concluded that the EDM method has two advantages over the conventional MOM: one is that the EDM method does not require evaluating the usual integrals involving the expansion and testing functions, thus reducing the computational complexity. Another is the reduction of the computation time for the calculations of each impedance matrix element, which can be obtained by one multiplication in the EDM method, while four multiplications in the conventional MOM using 1-point integration algorithm.

III. NUMERICAL RESULTS

In this section, three numerical results are presented to validate the algorithm and demonstrate the efficiency of the method. We remark that all the simulations are solved on a processor with 2.2GHz dual CPU speed. All coated structures are excited by a plane wave with the frequency of 0.3 GHz propagating along the –z direction.

In the first example, we consider a coated sphere shown in Fig. 2, where the electric dimension of the inner and outer spherical radius is $k_0a_1=0.2\pi$ and $k_0a_2=0.3\pi$, respectively, while the relative tensor elements of the uniaxial anisotropic material are $\varepsilon_{xx}=\varepsilon_{yy}=1.5-0.5j$, $\varepsilon_{zz}=2-j$, and $\mu_{xx}=\mu_{yy}=1.5-0.5j$, $\mu_{zz}=2-j$, the others are zero. The curves of Fig. 2 clearly show that the bistatic RCSs calculated in three different ways (the EDM method, the conventional MOM, HFSS) are in good agreement in both the xoz-plane and yoz-plane, thus validating the correctness and applicability of our method and the code.

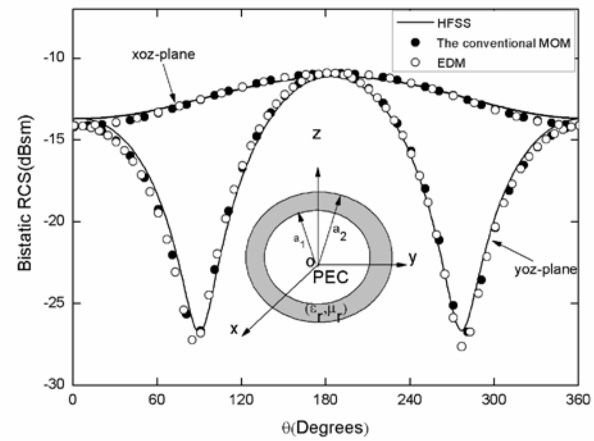

Fig. 2. Bistatic RCS of a conducting sphere coated with anisotropic uniaxial material.

Then, we consider a conducting sheet, which is coated with two-layer anisotropic materials. The relative tensor elements of the first layer sub1 are $\varepsilon_{xx}=\varepsilon_{yy}=1.5$, $\varepsilon_{zz}=2$, $\varepsilon_{xy}=j$, $\varepsilon_{yx}=-j$ and $\mu_{xx}=\mu_{yy}=\mu_{zz}=2-j$ and the others are zero. The relative tensor elements of the second layer sub2 are $\varepsilon_{xx}=\varepsilon_{yy}=\varepsilon_{zz}=2-j$ and $\mu_{xx}=\mu_{yy}=1.5$, $\mu_{zz}=2$, $\mu_{xy}=j$, $\mu_{yx}=-j$ and the others are zero. The configuration and its geometrical parameters are W=L=0.5m, $H_1=H_2=0.05$m, shown in Fig. 3. We remark here that the magnetic current unknowns could be paired with their corresponding electric current unknowns, thus resulting in total 6214 unknowns. The results of MOM are plotted in solid line, and the results of EDM are plotted in dotted line. It is observed that the results of the EDM method agree well with those of the conventional MOM, shown in Fig. 3. The total CPU time is 2249 seconds for EDM method and 4644 seconds for conventional method, respectively, which yields a reduction of 51.6% of the total computation time.

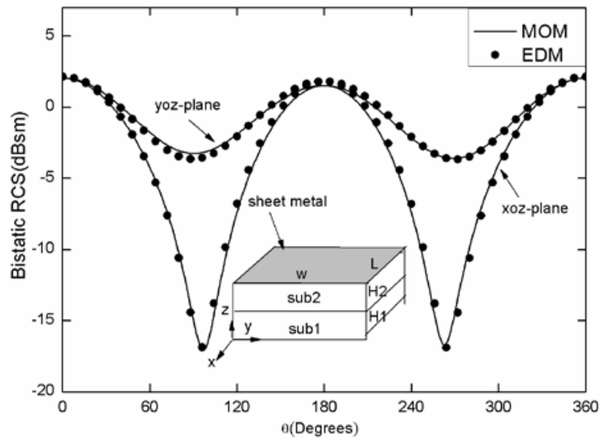

Fig. 3. Bistatic RCS of a metallic sheet coated with two-layer anisotropic off-diagonal materials.

In the last example, we consider the scattering from a coated connecting-ring, which is shown in Fig. 4 (a), and the geometrical parameters are D_1=100mm, D_2=150mm, D_3=200mm, D_4=500mm, H=500mm. The material of the coated layer of the model is uniaxial anisotropic lossy material with the relative tensors $\varepsilon_{xx} = \varepsilon_{yy} = 2 - j$, $\varepsilon_{zz} = 1.5 - 0.75j$ and $\mu_{xx} = \mu_{yy} = 1.5 - 0.75j$, $\mu_{zz} = 2 - j$, the others are zero. The unknowns (including triangles for perfect conductor and tetrahedrons for dielectric material) are 7011 in all. The RCS of the metallic connecting-ring coated with material is computed by both the conventional MOM (dashed line) and the EDM (dotted line), as shown in Fig. 4 (b) and (c), their results are in good agreement with each other. The total CPU time is 36915 seconds for conventional method and 24361 seconds for EDM method, respectively, which yields a reduction of 34% of the total computation time. We can also see from Fig. 4 (b) and (c), the presence of the uniaxial lossy material leads to the reduction of RCS in both xoz-plane and yoz-plane polarization in the scattering angle from 0° to 90° and 270° to 360° be about 7 dB lower than those of the metallic connecting-ring without coating material (solid line).

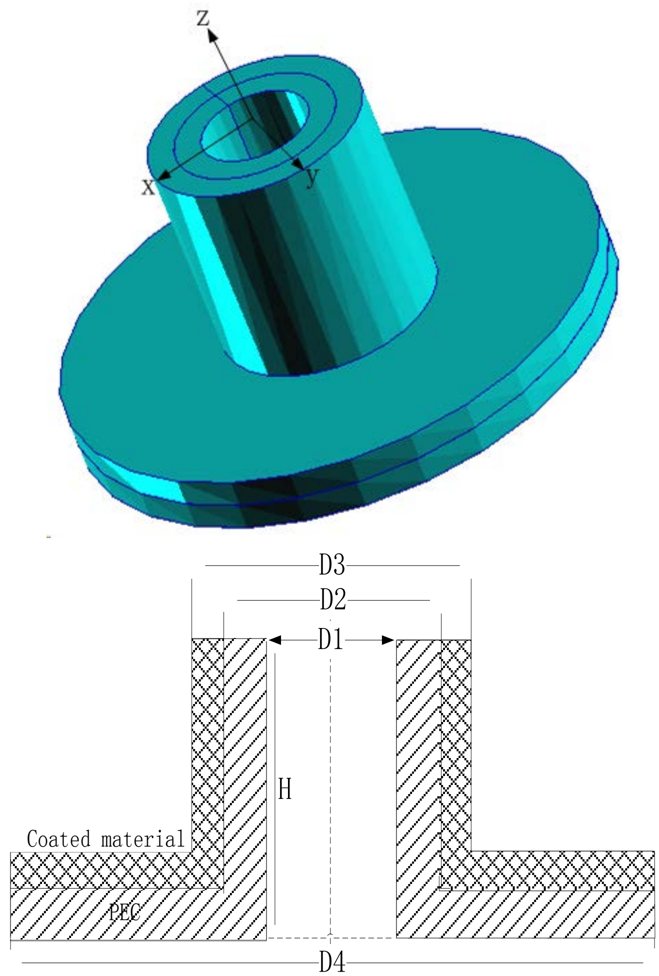

(a)

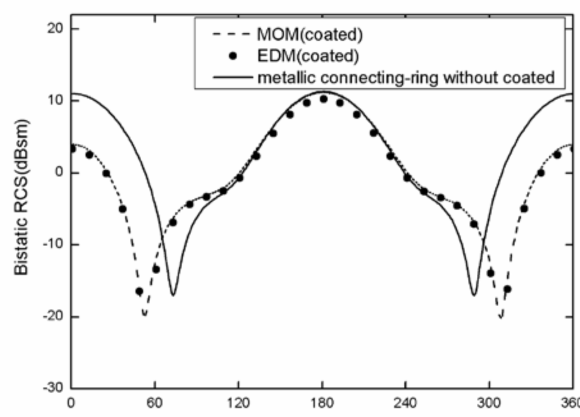

(b)

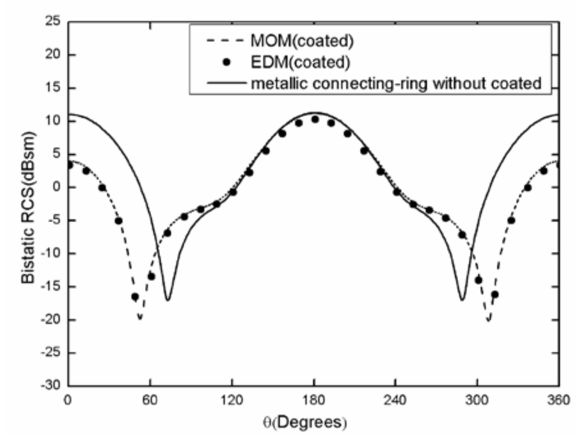

(c)

Fig. 4. (a) The connect-ring and its corresponding geometrical parameters, (b) bistatic RCS (xoz-plane) of a connecting-ring non-coated and coated with uniaxial material, (c) bistatic RCS (yoz-plane) of a connecting-ring non-coated and coated with uniaxial material.

IV. CONCLUSION

In this work, the EDM method has been successfully extended and applied in the analysis of the EM scattering characteristics of arbitrarily shaped PEC targets coated with arbitrary electric and magnetic anisotropic media. The application of the EDM method significantly reduces the computational complexity of the impedance matrix as well as the CPU time. All in all, the algorithm presented in this paper can be applied to analyze arbitrary shaped complex target coated with arbitrary thickness of EM anisotropic materials. In future work, we will focus on the application of the EDM method for the computation of the RCS of arbitrary shaped targets coated with bi-anisotropic materials.

ACKNOWLEDGMENT

The authors are grateful to Zhuo Li, Xinlei Chen and Ji Ding at College of Information Science and Technology, Nanjing University of Aeronautics and Astronautics, China, for their helpful suggestions and support during the project. The authors also gratefully acknowledge the support of the Joint Funding projects of the Aerospace Science Foundation Office of China and Nanjing University of Aeronautics and Astronautics (2008ZA52006).

REFERENCES

[1] Yin Hongcheng, Huang Peikang, and Liu Xueguan, “PO Solution for Scattering by the Complex Object Coated with Anisotropic Materials J-J,” *Journal of Systems Engineering and Electronics*, vol. 14, no. 2, pp.1-7, 2003.

[2] Z. Ruili, M. Zhizhou, L. Zha, et al., “FDTD Analysis of Wide-Band Scatting Characteristic of Metal Target Coated by Anisotropic Medium,” *Chinese Journal of Radio Science*, vol. 23, no. 1, pp. 11-16, 2008.

[3] Z. Xiuqin, G. Youlin, and W. Xinbao, “Application of MOM-CGM-FFT Method to Scattering from Three-Dimensional Magnetic Anisotropic Scatterers,” *Journal of microwave*, vol. 18, no. 3, pp. 7-13, June 2002.

[4] J. J. Angelin, “Hybrid Numerical Method for Harmonic 3-D Maxwell Equations: Scattering by a Mixed Conducting and Inhomogeneous Anisotropic Dielectric Medium [J],” *IEEE Transactions on Antennas and Propagation*, vol. 41, no. 1, pp. 66-76, 1993.

[5] G. Kobidze and B. Shanker, “Integral Equation Based Analysis of Scattering from 3-D Inhomogeneous Anisotropic Bodies,” *IEEE Transactions on Antennas and Propagation*, vol. 52, no. 10, pp. 2650-2658, October 2004.

[6] C. C. Su, “Electromagnetic Scattering by Dielectric Body with Arbitrary Inhomogeneity and Anisotropy,” *IEEE Transactions on Antennas and Propagation*, vol. 37, no. 3, pp. 384-389, March 1989.

[7] H. A. Sabbagh, R. K. Murphy, E. H. Sabbagh, et al., “The Joy of Computing with Volume Integrals: Foundations for Nondestructive Evaluation of Planar Layered Media,” *Applied Computational Electromagnetic Society (ACES) Journal*, vol. 25, no. 9, pp. 723-730, September 2010.

[8] C. Luo and C.-C. Lu, “Electromagnetic Scattering Computation Using a Hybrid Surface and Volume Integral Equation Formulation,” *Applied Computational Electromagnetic Society (ACES) Journal*, vol. 22, no. 3, pp. 340-349, November 2007.

[9] A. W. Glisson, M. Orman, F. Falco, et al., “Electromagnetic Scattering by an Arbitrarily Shaped Surface with an Anisotropic Impedance Boundary Condition,” *Applied Computational Electromagnetic Society (ACES) Journal*, vol. 10, no. 3, pp. 93-106, 1995.

[10] A. A. Kishk and P.-S. Kildal, “Electromagnetic Scattering from Two Dimensional Anisotropic Impedance Objects under Oblique Plane Wave Incidence,” *Applied Computational Electromagnetic Society (ACES) Journal*, vol. 10, no. 3, pp. 81-92, 1995.

[11] J. Yuan, C. Gu, and G. Han, "Efficient Generation of Method of Moments Matrices Using Equivalent Dipole-Moment Method," *IEEE Antennas and Wireless Propagation Letters*, vol. 8, pp. 716-719, 2009.

[12] J. Yuan, Z. Niu, Z. Li, et al., "Electromagnetic Scattering by Arbitrarily Shaped PEC Targets Coated with Anisotropic Media using Equivalent Dipole-Moment Method," *J Infrared Milli Terahz Waves*, vol. 31, no. 6, pp. 744–752, 2010.

[13] S. M. Rao, D. R. Wilton, and A. W. Glisson, "Electromagnetic Scattering by Surfaces of Arbitrary Shape," *IEEE Transactions on Antennas and Propagation*, vol. AP-30, no. 3, pp. 409-418, May 1982.

[14] D. H. Schaubert, D. R. Wilton, and A. W. Glisson, "A Tetrahedral Modeling Method for Electromagnetic Scattering by Arbitrarily Shaped Inhomogeneous Dielectric Bodies," *IEEE Transactions on Antennas and Propagation*, vol. AP-32, no. 1, pp. 77-85, January 1984.